J. Fluid Mech. (2006), *vol.* 558, *pp.* 319–328. © 2006 Cambridge University Press
doi:10.1017/S0022112006000383 Printed in the United Kingdom

Weak fountains

By N. B. KAYE AND G. R. HUNT

Department of Civil and Environmental Engineering, Imperial College London, Imperial College Road, London, SW7 2AZ, UK

(Received 27 January 2006 and in revised form 29 March 2006)

Analytical solutions for the initial rise height z_m of a turbulent fountain for the limits of both small and large source Froude number Fr_0 are presented. These solutions are based on a plume entrainment model. For large Froude number fountains, the established result $z_m/r_0 \sim Fr_0$ is obtained (r_0 denoting the source radius). For intermediate Froude numbers, the relationship $z_m/r_0 \sim Fr_0^2$ is found and the rise height is independent of the entrainment coefficient α. For very small Froude numbers, the flow is hydraulically controlled at the source and $z_m/r_0 \sim Fr_0^{2/3}$. Existing experimental and numerical results, as well as our own experimental results, are compared to our solutions and show good agreement. Comparison with experimental results also demonstrates that the appropriate entrainment coefficient for highly forced fountains is $\alpha_f \approx 0.058$. This is significantly closer to the entrainment coefficient of a jet than of a plume.

1. Introduction

Turbulent fountains are formed by the continuous high-Reynolds-number steady supply of buoyant fluid to a quiescent environment with a source momentum flux that opposes the buoyancy flux. A schematic of the flow development of a turbulent fountain is shown in figure 1. A negatively buoyant fountain will rise upward, owing to the source momentum flux, and entrain ambient fluid (figure 1*a*). However, the opposing buoyancy force acts to reduce the local momentum flux, resulting in the fountain stopping at the initial maximum rise height z_m (figure 1*b*). The flow then reverses direction and falls back down around the up-flowing fountain core, settling at a steady-state height z_{ss} that is approximately 30 % below the initial maximum (figure 1*c*).

Using dimensional arguments, Turner (1966) showed that the rise height of a fountain scales on the source momentum jet length (Morton 1959)

$$z_m \sim L_M(z=0) = \left(\frac{5M_0^{3/2}}{9\alpha F_0}\right)^{1/2}, \tag{1.1}$$

where the source momentum flux is given by $\pi M_0/2$, the source buoyancy flux by $\pi F_0/2$ and the entrainment coefficient by α. (Herein the momentum jet length is written in the same way as in Hunt & Kaye (2005), rather than in Turner (1966), for consistency with the analytical model presented in § 2.)

Turner (1966) presented experimental results that showed that both the initial rise height (z_m) and the steady-state rise height (z_{ss}) scale on $L_M(0)$ with

$$z_m \approx 1.43 z_{ss}. \tag{1.2}$$

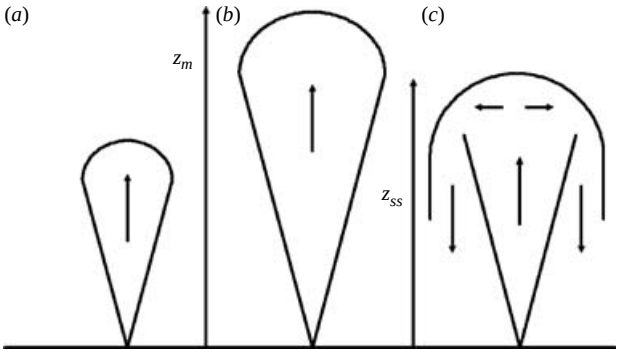

FIGURE 1. Schematic of a turbulent fountain rising owing to source momentum flux (*a*), reaching peak height (*b*) and settling to steady-state height (*c*).

Again using dimensional arguments, Baines, Turner & Campbell (1990) scaled the rise height on the source radius (r_0) and showed that this dimensionless rise height is a linear function of the source Froude number $Fr_0 = u_0/\sqrt{r_0 g_0'}$, where the subscript '0' refers to values at the source and u and g' are the vertical velocity and reduced gravity, respectively. Note that $Fr_0 \sim L_M(0)/r_0$ implying the same jet length scaling as Turner (1966). Baines *et al.* (1990) extended the range of Froude numbers covered by the experiments of Turner (1966) to $Fr_0 \approx 250$ and their experimental results confirmed that

$$\frac{z_{ss}}{r_0} = 2.46 Fr_0. \tag{1.3}$$

Lane-Serff, Linden & Hillel (1993) also parameterized the rise height in terms of the jet length when examining forced angled plumes. Furthermore, they showed that the flow could be described in terms of a point source of momentum and buoyancy located at a virtual origin. (In our formulation of the equations described later we parameterize the flow in terms of a source parameter Γ_0 (2.2) which has an ambiguous limit at the virtual origin. $\Gamma_0 = 0$ can represent a zero volume flux or zero buoyancy flux source. Therefore, our formulation does not lead to a virtual origin correction.)

Bloomfield & Kerr (2000) present a theoretical model for the rise height of a fountain. They modified the plume entrainment equations of Morton, Taylor & Turner (1956) to account for the down-flow on the steady-state rise height. Their model accounted for entrainment between the up-flow and down-flow as well as between the down-flow and the ambient. Bloomfield & Kerr (2000) varied the rate of entrainment for each of these areas of fluid exchange and found that z_{ss} is sensitive only to the entrainment rate between the down-flow and the ambient fluid. By reducing this entrainment, the down-flow remains relatively more dense and, therefore, gains momentum. This would seem to imply that the most significant factor in reducing the rise height from peak (z_m) to steady state (z_{ss}) is the entrainment of downward momentum into the upward flowing fountain.

'Weak' turbulent fountains, that is, fountains with small source Froude numbers, were examined by Zhang & Baddour (1998). They present experimental results for the initial penetration depth z_m of a fountain for $0.37 \leqslant Fr_0 \leqslant 36.2$. Their experimental results indicate that for $Fr_0 < 7$, the linear Froude number scaling does not apply and the appropriate scaling is $z_m/r_0 \sim Fr_0^{1.3}$. However, Lin & Armfield (2000*a*) present numerical simulation data in the range $0.1 \leqslant Fr_0 \leqslant 1.0$ that suggests the linear Froude number scaling is valid, but for $Fr_0 > 1$ this relationship will underestimate

the rise height. They, therefore, regard weak fountains as those with source Froude numbers less that one. This work was extended by Lin & Armfield (2000*b*) to very weak fountains where viscosity plays a role. They argue that for very weak fountains, the only parameters that play a role are the viscosity ν and the source buoyancy g_0'. Therefore

$$z_m \sim \left(\frac{\nu^2}{g_0'}\right)^{1/3} \quad \text{or} \quad \frac{z_m}{r_0} \sim \left(\frac{Fr_0}{Re_0}\right)^{2/3}. \tag{1.4}$$

This leads to the counter-intuitive result that the rise height increases with decreasing Reynolds number Re_0. Their numerical simulation results support their Froude-number scaling (for example their equation (26) gives $z_m/r_0 = 1.26Fr_0^{2/3}$, for $Re_0 = 200$); however, their Reynolds number results are less clear. For $Fr_0 = 0.05$, they obtain $z_m/r_0 = 0.1615 + 0.3803Re_0^{-2/3}$ (their equation (28)). For $Re_0 > 50$, the Reynolds-number term accounts for less than 15 % of the rise height and the constant term dominates. It would therefore appear that the flow need not be fully turbulent for the Reynolds-number effect to be small.

Clearly there is some disagreement in the literature regarding weak turbulent fountains. It is the goal of this paper to determine the exact nature of the rise height scaling for weak turbulent fountains, to establish the range of Froude numbers for which fountains should be regarded as weak and to explain the role of the Reynolds number on the rise height.

In § 2, the plume conservation equations of Morton *et al.* (1956) are rewritten in the form introduced by Hunt & Kaye (2005). Analytic solutions are then presented for the initial rise height of a fountain for both small and large Froude-number limits. However, for very small Froude numbers, our model is no longer appropriate as the flow is hydraulically controlled at the source. In this case, we present a physical argument for the Froude-number scaling and discuss the role of viscosity. In § 3, these solutions are compared to new and existing experimental and numerical results. When scaled, all these results collapse onto a single line covering three separate regimes of 'forced', 'weak' and 'very weak' fountains. Based on these results, the appropriate entrainment coefficient for a large-Froude-number highly-forced turbulent fountain is discussed. Conclusions are drawn in § 4.

2. Analytic solutions for initial rise height

The conservation equations of Morton *et al.* (1956) for a constant buoyancy flux plume from a localized horizontal source in a quiescent uniform environment can be written in terms of the fluxes of volume (πQ), momentum and buoyancy as

$$\frac{\mathrm{d}Q}{\mathrm{d}z} = 2\alpha M^{1/2}, \qquad \frac{\mathrm{d}M}{\mathrm{d}z} = 2\frac{QF}{M}, \tag{2.1}$$

where α is the entrainment coefficient appropriate for Gaussian profiles and z is the vertical coordinate measured from the source. In general, the source conditions are $Q = Q_0$, $M = M_0$ and $F = F_0$ at $z = 0$. For a fountain, M_0 is positive when in the positive z-direction and, therefore, F_0 will be negative. Although these equations are only strictly applicable to fully developed self-similar flows, they have been successfully applied to non-self-similar flows such as a plume in a stratified environment (Morton *et al.* 1956), highly forced plumes (Morton 1959), highly lazy plumes (Hunt & Kaye 2001) and turbulent fountains (Bloomfield & Kerr 2000).

Hunt & Kaye (2005) showed that (2.1) can be rewritten in terms of the flux balance parameter Γ and the dimensionless plume (or fountain) radius β

$$\Gamma(z) = \frac{5Q(z)^2F(z)}{4\alpha_{jet}M(z)^{5/2}}, \qquad \beta(z) = \frac{Q(z)M(z)^{-1/2}}{Q_0M_0^{-1/2}}. \tag{2.2}$$

Hunt & Kaye (2005) use a constant entrainment coefficient α in their model. However, this is unlikely to be the case for flows that are not fully self-similar (see Kaminski, Tait & Carazzo 2005). We therefore write $\phi = \alpha/\alpha_{jet}$ in our model. The equations of Hunt & Kaye (2005) now become

$$\frac{\mathrm{d}\Gamma}{\mathrm{d}\zeta} = \frac{10\Gamma}{3\beta}(\phi - \Gamma), \qquad \frac{\mathrm{d}\beta}{\mathrm{d}\zeta} = \tfrac{1}{3}(5\phi - 2\Gamma), \tag{2.3}$$

where $\zeta = z/(5Q_0/6\alpha_{jet}M_0^{1/2})$. Although we will not present solutions for a variable α flow, we write the equations in this way to demonstrate the role of α in the various flow regimes. Note that Γ is equivalent to the Richardson (Ri) number, or the inverse square of the Froude number $\Gamma \sim Ri \sim Fr^{-2}$.

For a fountain, the source buoyancy flux and momentum flux are of opposite sign. The source value of Γ is therefore negative and for convenience we write $\Gamma' = -\Gamma$ such that $\Gamma' > 0$. (2.3) then becomes

$$\frac{\mathrm{d}\Gamma'}{\mathrm{d}\zeta} = \frac{10\Gamma'}{3\beta}(\phi + \Gamma'), \qquad \frac{\mathrm{d}\beta}{\mathrm{d}\zeta} = \tfrac{1}{3}(5\phi + 2\Gamma'), \tag{2.4}$$

which can only be applied to the initial rise of the fountain and not to the subsequent collapse of the flow. The source conditions are given by

$$\Gamma' = \Gamma'_0, \qquad \beta = 1 \quad \text{at} \quad \zeta = 0. \tag{2.5}$$

Any non-zero finite positive value of Γ' will lead to a growth in Γ' with height (2.4). Also, as $\Gamma' \to \infty$ the value of $\beta \to \infty$. Therefore, it is assumed that the fountain will reach its maximum height in this limit.

Equation (2.4) can be solved subject to (2.5) to give the width

$$\beta = \frac{\Gamma'^{1/2}}{(\phi + \Gamma')^{3/10}} \frac{(\phi + \Gamma'_0)^{3/10}}{\Gamma_0'^{1/2}}. \tag{2.6}$$

Equation (2.4) can now be rewritten as

$$\frac{\mathrm{d}\Gamma'}{\mathrm{d}\zeta} = \frac{10}{3} \frac{\Gamma_0'^{1/2}}{(\phi + \Gamma'_0)^{3/10}} \Gamma'^{1/2}(\phi + \Gamma')^{13/10}. \tag{2.7}$$

The initial rise height of the fountain ζ_m is therefore

$$\zeta_m = \frac{3}{10} \frac{(\phi + \Gamma'_0)^{3/10}}{\Gamma_0'^{1/2}} \int_{\Gamma'_0}^{\infty} \Gamma'^{-1/2}(\phi + \Gamma')^{-13/10}\,\mathrm{d}\Gamma'. \tag{2.8}$$

2.1. *Highly forced fountains*

For highly forced fountains, that is, large Fr_0 or $\Gamma'_0 \ll 1$, we make the assumption that $\phi + \Gamma'_0 \approx \phi \approx 1$. The assumption that $\phi \approx 1$ for small Γ' is reasonable as the flow will be dominated by the source momentum flux, buoyancy will play only a minor role and the flow will behave as a jet. Our assumption will only be valid up to some value of $\Gamma'(z) = \Gamma'_{lim} (> \Gamma'_0)$ beyond which the full expression (2.8) must be solved.

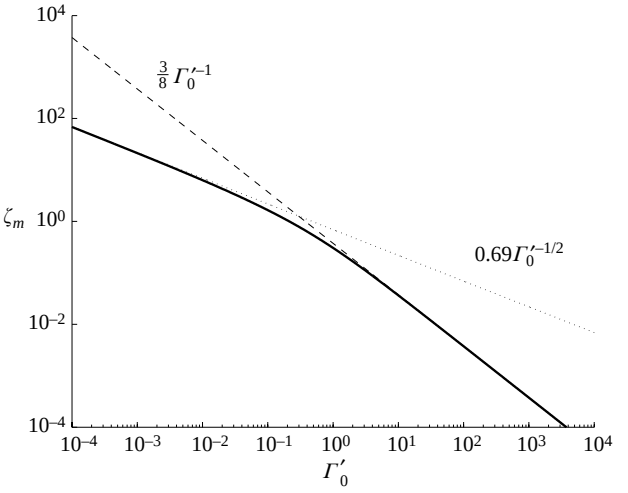

FIGURE 2. Log–log plot of the initial rise height ζ_m as a function of the source condition Γ_0' showing the numerical solution of (2.8) (thick line), weak fountain analytic solution (2.14) (dashed line), and derived power-law solution for highly forced fountains (2.12) (dotted line).

The rise height is therefore

$$\zeta_m \approx \frac{3}{10\Gamma_0'^{1/2}} \left(\int_{\Gamma_0'}^{\Gamma_{lim}'} \Gamma'^{-1/2}\, \mathrm{d}\Gamma' + \phi^{3/10} \int_{\Gamma_{lim}'}^{\infty} \Gamma'^{-1/2} (\phi + \Gamma')^{-13/10} \mathrm{d}\Gamma' \right). \tag{2.9}$$

The second integral is independent of the source value Γ_0' and we write

$$I = \phi^{3/10} \int_{\Gamma_{lim}'}^{\infty} \Gamma'^{-1/2} (\phi + \Gamma')^{-13/10}\, \mathrm{d}\Gamma'. \tag{2.10}$$

The solution for ζ_m is therefore

$$\zeta_m \approx \frac{3}{5} \left[\left(\frac{\Gamma_{lim}'}{\Gamma_0'} \right)^{1/2} - 1 + \frac{I}{2\Gamma_0'^{1/2}} \right]. \tag{2.11}$$

In the limit of very small Γ_0' such that $\Gamma_{lim}'/\Gamma_0' \gg 1$, (2.11) leads to a scaling for the rise height in terms of Γ_0' of $\zeta_m \sim \Gamma_0'^{-1/2} - C$. This is the same linear Froude-number scaling as in Baines *et al.* (1990), but with a constant offset C. The linear Froude-number scaling is therefore only applicable in the limit of highly forced fountains where Fr_0 is considerably greater than C. This is because highly forced fountains rise like jets for small ζ, but as ζ increases, the buoyancy force reduces the momentum flux, the fountain becomes weaker (Γ' increases) and the flow moves into a regime with a different rise height scaling (see figure 2). In other words, the linear Froude-number scaling is only applicable when the vast majority of the rise height is attained in the highly forced regime.

Numerical solutions of (2.8) with $\phi = 1$ calculated over a wide range of Γ_0' are shown in a log–log plot in figure 2. This figure shows two power-law relationships, one for small values of Γ_0' (large-Froude-number highly forced fountains) and another for larger values of Γ_0' (small-Froude-number weak fountains). The transition between the two regimes occurs around $\Gamma_0' = O(1)$. In the limit of very small Γ_0', that is, very

large Froude number, we can approximate the rise height as

$$\zeta_m \approx 0.69 \Gamma_0'^{-1/2}, \tag{2.12}$$

based on a fit of the numerical solution of the form $\zeta_m \sim \Gamma_0'^{-1/2}$.

2.2. *Weak fountains*

For weak fountains, that is small Fr_0 or $\Gamma_0' \gg \phi$, we make the simplifying approximation that $\phi + \Gamma' \approx \Gamma'$. For large Γ' flows, variable entrainment models predict that α will be reduced, that is $\phi < 1$. However, (2.4) indicates that the entrainment becomes insignificant in the flow development ($\Gamma' \gg \phi$) even if it is constant, and the reduced entrainment will not effect the analytical results as ϕ is negligibly small compared with Γ'. Equation (2.8) can now be approximated by

$$\zeta_m \approx \tfrac{3}{10} \Gamma_0'^{-1/5} \int_{\Gamma_0'}^{\infty} \Gamma'^{-9/5} \, \mathrm{d}\Gamma'. \tag{2.13}$$

The initial rise height is therefore

$$\zeta_m \approx \tfrac{3}{8} \Gamma_0'^{-1}. \tag{2.14}$$

This result approaches the exact solution as $\Gamma_0' \to \infty$. For weak fountains, (2.14) implies that the rise height scales on the square of the Froude number, rather than linearly as for forced fountains (1.3). The rise height therefore scales on $z_m \sim u_0^2/g_0'$ rather than on the momentum jet length $L_M(0)$. This implies that the energy of the flow is conserved with the source kinetic energy completely converted into potential energy. Note also that entrainment will be reduced and the flow will not be fully developed. The central core flow of the fountain will be unaffected by the ambient fluid this close to the source.

The analytic solution for weak fountains (2.14) and the power-law scaling derived for forced fountains (2.12) are plotted in figure 2. The relative error

$$\varepsilon = \left. \frac{(\mathrm{d}\Gamma'/\mathrm{d}\zeta)_{approx}}{(\mathrm{d}\Gamma'/\mathrm{d}\zeta)_{exact}} \right|_{\Gamma' = \Gamma_0'}, \tag{2.15}$$

associated with our small and large Γ' approximations can be used to estimate the value of Γ' for which the flow will move from the forced to the weak regime. We assume that this transition occurs when the relative error ε is equal for both approximations. This occurs at $\Gamma_0' = 1$.

2.3. *Very weak fountains*

For very weak fountains the problem becomes one of hydraulic control. The steady-state height of the fountain provides the head required to drive the fountain outflow radially over the nozzle edge (see figure 3). The outflow will be at the critical depth ($Fr_{out} = 1$, $z = z_c = 2z_{ss}/3$) as for flow over a weir and, therefore, $v_{out} = \sqrt{z_c g_0'}$. Conservation of volume requires that

$$2\pi r_0 z_c v_{out} = \pi r_0^2 u_0 \quad \text{or} \quad \frac{z_{ss}}{r_0} \approx 0.94 Fr_0^{2/3}. \tag{2.16}$$

This is the same Froude-number scaling as in Lin & Armfield (2000*b*). This model (2.16) also explains the role of the Reynolds number on the flow rise height. As viscosity becomes more significant it will create a drag on the outflow. This will increase the amount of energy required to drive the flow. The energy can only be supplied by increasing the head, that is increasing the steady-state rise height of

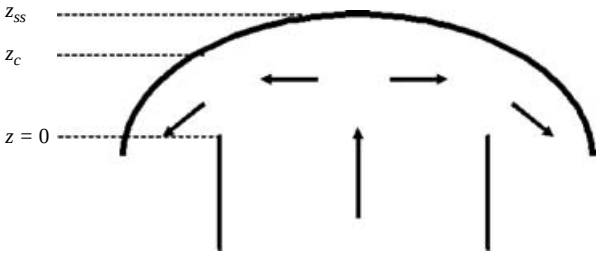

FIGURE 3. Schematic of a vertical section through the fountain nozzle showing the radial outflow from the fountain controlled by the critical depth at the nozzle edge.

the fountain. Equation (2.16) therefore provides a lower bound on the rise height for very weak fountains, that is the rise height for large-Reynolds-number flow. For lower-Reynolds-number flow, the rise height will be greater.

3. Comparison of model with experiments

There are already extensive data sets on the rise height of fountains from both experimental (Baines *et al.* 1990) and numerical (Lin & Armfield 2000*a*, *b*) studies. In this section, we re-plot this data on a log–log plot of steady-state rise height scaled on the source radius (z_{ss}/r_0) against the source Froude number (Fr_0). Although our theoretical predictions are only for the initial rise height, it is reasonable to expect that the power-law scalings will hold for both the rise and settling heights.

Small-scale laboratory experiments were also performed to supplement the existing data on the steady rise height of weak turbulent fountains. The fountains were formed by forcing a dense saline solution vertically upward into a large tank of still fresh water. The saline solution was dyed with food colouring and the experiment was diffusively back lit. The experiments were recorded using a CCD camera connected to the DigiFlow image processing software (Dalziel 1993). The source volume flow rate and radius were varied in order to change the source Froude number. Owing to the physical constraints of the experimental set-up, it was not possible to systematically study the influence of the Reynolds number on the experimental results. This work focused on the intermediate Froude number regime – that is, Froude numbers between the hydraulically controlled and highly forced regimes. Data from the very weak and highly forced regimes are plotted to demonstrate the consistency of our experimental results with existing fountain data. A time series of typical images from our experiments is shown in figure 4.

Our experimental data, along with the experimental data from Baines *et al.* (1990) and the numerical data from Lin & Armfield (2000*a*), are plotted in figure 5. For small Fr_0, it was difficult to read the data accurately from figure 6 of Baines *et al.* (1990). We therefore plot their data only for $Fr_0 > 10$. The data show good agreement with the result for intermediate Froude numbers, namely, that the rise height scales on the square of the Froude number, not linearly, as is the case for large Froude numbers. The theoretical result (2.16) also provides a lower bound on the rise height, as predicted. Our experimental apparatus did not allow for a full exploration of the Reynolds-number dependence for very weak fountains. However, the model presented does give a physical explanation for the result of Lin & Armfield (2000*b*) that the rise height increases with decreasing Reynolds number.

FIGURE 4. Series of images taken at 24 frames per second from a typical experiment with a weak fountain. The source conditions were $Fr_0 = 1.3$ and $Re_0 = 254$.

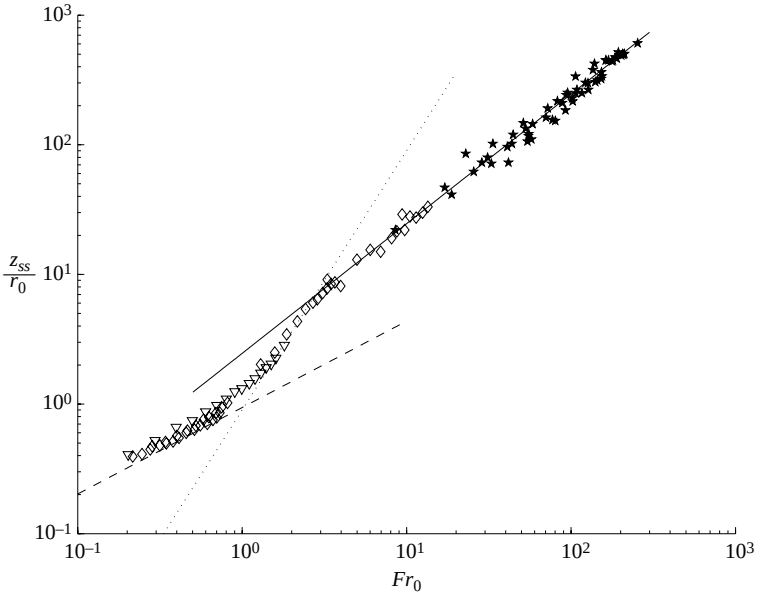

FIGURE 5. Experimental results for the steady-state rise height z_{ss} as a function of the source Froude number. The solid line is given by $z_{ss}/r_0 = 2.46Fr_0$, the dashed line by $z_{ss}/r_0 = 0.94Fr_0^{2/3}$ and the dotted line by $z_{ss}/r_0 = 0.9Fr_0^2$. The symbols represent data from: $\star$, Baines *et al.* 1990; ∇, Lin & Armfield 2000*a*; $\diamond$, our experiments conducted for this paper.

The question of transition Froude numbers is complex owing to the role of viscosity at low Froude number. It would appear from figure 5 that the transition from highly forced to weak fountains occurs at $Fr_0 \approx 3$. The transition from weak to very weak fountains will be dependent on both the Froude number and Reynolds number. In the limit when viscosity does not play a role, the transition will occur at $Fr_0 \approx 1$, as predicted by Lin & Armfield (2000*b*). This transition Froude number will increase with decreasing Re_0. We can therefore write the steady-state rise height for an axisymmetric fountain as

$$\frac{z_{ss}}{r_0} \approx \begin{cases} 2.46Fr_0 & \text{for} \quad Fr_0 \gtrsim 3, \\ 0.90Fr_0^2 & \text{for} \quad 1 \lesssim Fr_0 \lesssim 3, \\ 0.94Fr_0^{2/3} & \text{for} \quad 0 < Fr_0 \lesssim 1. \end{cases} \tag{3.1}$$

For weak fountains, we have shown that the rise height is independent of α. However, this is not true for high-Froude-number flows. A question then arises as to what is the most appropriate value of α for a fountain. Entrainment is largely due to engulfing of ambient fluid by the largest vortex-like structures in the flow. In buoyancy-driven flows, the vorticity has two main sources, shear and baroclinic torque. In a plume, the shear and baroclinic torques act together and result in a larger entrainment coefficient than is produced by shear alone. Hence, plumes have a higher measured entrainment coefficient than jets. In fountains, the baroclinic torque opposes the shear, and we might expect α to be less than either that of a jet or that of a plume. However, for highly forced (large-Froude-number) fountains the bulk of the rise height is attained while the momentum-driven jet flow dominates and the opposing buoyancy force plays only a minor role. Therefore, we might expect that for a highly forced fountain, $\alpha_f \approx \alpha_{jet}$. We can estimate α_f by comparing our experimental and theoretical results in the limit of large Fr_0. Rearranging (2.12), we obtain $z_m/r_0 = 0.87Fr_0/\sqrt{\alpha_f}$. We can directly compare this expression with (1.3) using the result (1.2) from Turner (1966) to obtain $z_{ss}/r_0 = 2.46Fr_0 = 0.852Fr_0/1.43\sqrt{\alpha_f}$ or $\alpha_f = 0.058$. This is very close to the value $\alpha_{jet} = 0.0535$ (see Fischer *et al.* 1979). For smaller Froude numbers, we might expect the entrainment coefficient to be a function of the Froude number in a manner similar to that for plumes, as shown by Kaminski *et al.* (2005). A detailed analysis of this problem is beyond the scope of this paper.

Now that we have an estimate of α_f, we can compare values of Γ_0' to Fr_0. Γ_0' written in terms of the source velocity, buoyancy and radius is

$$\Gamma_0' = \frac{5r_0 g_0'}{2^{7/2}\alpha_f u_0^2} = \frac{5}{2^{7/2}\alpha_f} Fr_0^{-2}. \tag{3.2}$$

Substituting $\alpha_f = 0.058$ and our earlier estimate of the highly forced to weak transition value of $\Gamma_0' = 1$, we estimate that the transition to the weak regime occurs at $Fr_0 = 2.8$. This is in very good agreement with our experimental results that indicated a transition for $Fr_0 \approx 3$.

4. Conclusions

We have recast the plume conservation equations of Morton *et al.* (1956) in terms of the dimensionless parameter $\Gamma(z) \sim Fr(z)^{-2}$ and dimensionless flow width $\beta(z)$, and solved for the initial rise height of a fountain over a range of source Froude numbers. We demonstrate that for intermediate Froude numbers ($1 \lesssim Fr_0 \lesssim 3$) the rise height of the fountain no longer scales linearly on Fr_0 but rather on Fr_0^2. The rise height also becomes independent of the entrainment coefficient α. This result may have a significant impact on the parameterization of the entrainment across density interfaces driven by turbulence in plume-, jet- or fountain-like flows. For $Fr_0 \lesssim 1$, the flow is hydraulically controlled by the radial outflow and the rise height scales on $z_{ss}/r_0 \sim Fr_0^{2/3}$. In this regime, viscosity will tend to retard the outflow, which then requires an increased head to drive it. Therefore, the fountain rise height will increase with decreasing Reynolds number.

A series of laboratory experiments was conducted to identify the existence of the weak-fountain flow regime and to verify the $z_{ss}/r_0 \sim Fr_0^2$ power-law scaling we derived. Our experimental results are plotted, together with previously published data. Our experimental results are consistent with these sets of data, and clearly show the intermediate flow regime where $z_{ss}/r_0 \sim Fr_0^2$. The hydraulic control model for very weak fountains provides a lower bound on their rise height. We also use the rise height

limit for large-Froude-number fountains of Baines *et al.* (1990) to establish that the appropriate entrainment coefficient of a highly forced fountain is approximately equal to that of a pure jet.

N. B. K. and G. R. H. would like to thank the EPSRC and BP Advanced Energy Programme at Imperial College London for their support of this research, and Dr Greg Lane-Serff for his help with the very weak fountain regime.

REFERENCES

Baines, W. D., Turner, J. S. & Campbell, I. H. 1990 Turbulent fountains in an open chamber. *J. Fluid Mech.* **212**, 557–592.

Bloomfield, L. J. & Kerr, R. C. 2000 A theoretical model of a turbulent fountain. *J. Fluid Mech.* **424**, 197–216.

Dalziel, S. B. 1993 Rayleigh–Taylor instability: experiments with image analysis. *Dyn. Atmos. Oceans* **20**, 127–153.

Fischer, H. B., List, E. J., Koh, R. C. Y., Imberger, J. & Brooks, N. H. 1979 *Mixing in Inland and Coastal Waters*. Academic.

Hunt, G. R. & Kaye, N. B. 2005 Lazy plumes. *J. Fluid Mech.* **533**, 329–338.

Hunt, G. R. & Kaye, N. G. 2001 Virtual origin correction for lazy turbulent plumes. *J. Fluid Mech.* **435**, 377–396.

Kaminski, E., Tait, S. & Carazzo, G. 2005 Turbulent entrainment in jets with arbitrary buoyancy. *J. Fluid Mech.* **526**, 361–376.

Lane-Serff, G. F., Linden, P. F. & Hillel, M. 1993 Forced, angled plumes. *J. Hazard. Mat.* **33**, 75–99.

Lin, W. & Armfield, S. W. 2000*a* Direct simulation of weak axisymmetric fountains in a homogeneous fluid. *J. Fluid Mech.* **403**, 67–88.

Lin, W. & Armfield, S. W. 2000*b* Very weak fountains in a homogeneous fluid. *Numer. Heat Transfer* A **38**, 377–396.

Morton, B. R. 1959 Forced plumes. *J. Fluid Mech.* **5**, 151–163.

Morton, B. R., Taylor, G. I. & Turner, J. S. 1956 Turbulent gravitational convection from maintained and instantaneous sources. *Proc. R. Soc. Lond.* A **234**, 1–23.

Turner, J. S. 1966 Jets and plumes with negative or reversing buoyancy. *J. Fluid Mech.* **26**, 779–792.

Zhang, H. & Baddour, R. E. 1998 Maximum penetration depth of vertical round dense jets at small and large Froude number. *J. Hydraul. Div. Proc. ASCE* **124**, 550–553.